

**The Pseudouridine Synthases Proceed through a Glycol Intermediate**

Govardhan Reddy Veerareddygar, Sanjay K. Singh, and Eugene G. Mueller\*

Department of Chemistry, University of Louisville, Louisville, KY 40205

**Experimental Section**

**General.** All standard chemicals, unless specified were purchased from Fisher Scientific (Pittsburgh, PA) or Sigma Aldrich (Milwaukee, WI). Oligonucleotides (RNA) were obtained from GE Dharmacon (Lafayette, CO), deprotected according to the manufacturer's protocol, and purified by HPLC. Oligodeoxynucleotides (DNA) were purchased from Integrated DNA Technologies (Coralville, IA). Deuterium oxide (99.9%) was obtained from Cambridge Isotope Laboratories, Inc. (Tewksbury, MA). Y76L TruB was generated *in silico* and energy-minimized using the GROMOS 43B1 force field<sup>1</sup> as implemented in Swiss-Pdb Viewer v4.0.<sup>2</sup> PyMOL v1.3 was used to generate high-resolution graphics of these structures.<sup>3</sup> [<sup>2</sup>-<sup>3</sup>H]ribose was purchased from Omicron Biochemicals, Inc. (South Bend, IN). Restriction endonucleases *Nde*I and *Bam*HI and thermostable inorganic pyrophosphatase were purchased from New England BioLabs (Ipswich, MA). Modified chymotrypsin (sequencing grade) was purchased from Roche (Indianapolis, IN), and immobilized pepsin was purchased from Fisher Scientific (Waltham, MA). Phosphoenolpyruvate (PEP) was purchased from Chem-Impex International (Wood Dale, IL). Pyruvate kinase/lactate dehydrogenase enzyme cocktail, pyruvate kinase II from rabbit muscle, ribose 5-phosphate barium salt (R5P•Ba), Dowex-50 (H<sup>+</sup> form), and Norit® and Darco G-60 activated charcoal were obtained from Sigma Aldrich (Milwaukee, WI). Dowex-50 (H<sup>+</sup> form) was cleaned by the method of Cleland.<sup>4</sup> Prior to use, the activated charcoal (2 g) was mixed with 0.01 N HCl (30 mL); the mixture was centrifuged (8000g, 15 min), and the supernatant was discarded. Yeast myokinase was purchased from CalBiochem (BillERICA, MA). Amicon DIAFLO ultrafiltration units were purchased from Millipore Corporation (Bedford, MA). Bond Elut C8 solid phase extraction cartridges (5 g, 20 mL) were obtained from Agilent Technologies (Santa Clara, CA). Ribonucleotide triphosphates (rNTPs) were purchased from Promega (Madison, WI), and T7 RNA polymerase was purchased from Epicentre biotechnologies (Madison, WI). Stop RNase Inhibitor RX was purchased from 5 PRIME, Inc. (Gaithersburg, MD), and TURBO™ DNase was purchased from Life Technologies (Carlsbad, CA). Phosphoribosyl pyrophosphate (PRPP) was freshly isolated by the method of Gross et al.<sup>5</sup> All coupled enzymatic activity assays were performed with a DU 800 Series UV/Vis spectrophotometer (Beckman Coulter; Pasadena, CA) equipped with a six cell transporter and a Peltier temperature controller. NMR spectra were acquired using a 400-MR spectrometer equipped with a 5 mm direct HX z-PFG broadband probe (Varian Inc., Palo Alto, CA).

**RNA substrates, products, and reaction buffers.** As described previously, TruB and RluA efficiently handle stem-loop RNAs (17-mers).<sup>6,7</sup> The canonical 17-mer substrate for TruB is the T-arm stem-loop (TSL) of yeast tRNA<sup>Phe</sup>, CUGUGUUCGAUCCACAG, and that for RluA is the anticodon stem-loop (ASL) of *E. coli* tRNA<sup>Phe</sup>, GGGGAUUGAAAAUCCCC; the isomerized U is underlined. The stem-loops in which the isomerized U is substituted with 5-fluorouridine (F<sup>5</sup>U) are denoted [F<sup>5</sup>U]TSL and [F<sup>5</sup>U]ASL. TruB reaction buffer is 50 mM HEPES buffer, pH 7.5, containing ammonium chloride

(100 mM), EDTA (1 mM), and DTT (5 mM), and RluA reaction buffer is the same except that ammonium chloride is replaced with sodium chloride (175 mM). The hydrated, rearranged products of F<sup>5</sup>U are denoted as F<sup>5</sup>U\*; they are isolated as dinucleotides with the following nucleoside in the parent RNA (F<sup>5</sup>U\*pC from [F<sup>5</sup>U]TSL and F<sup>5</sup>U\*pU from [F<sup>5</sup>U]ASL).<sup>8,9</sup> For the purposes of the experiments reported here, the dinucleotide nature of the products is unimportant and will not typically be noted in the text.

**Overexpression and purification of Y76L TruB.** The plasmid encoding Y76L TruB (pUL323) was created by introducing a point mutation into *truB* (from *E. coli*) in pY55<sup>9,10</sup> using a Stratagene QuickChange™ site-directed mutagenesis kit using the manufacturer's protocols with the following primers: 5'-GACTCCGACAAAGGTCTCCGGGTCATTGCG-3' (forward), and 5'-CTGTC-CAAGACGCGCAATGACCCGG-3' (reverse); the positioning and sequence of the insert in the resulting pUL323 was verified by DNA sequencing. BLR(DE3) pLysS cells were transformed with pUL323 for the overexpression of Y76L TruB. Overexpressed Y76L TruB was purified over Ni-NTA resin (QIAGEN, Valencia, CA) using the same protocol used for wild-type TruB.<sup>10</sup> Subsequently, Y76L TruB was polished over a POROS HQ anion exchange column (PE Biosystems) attached to a BioCAD SPRINT FPLC run by Perfusion Chromatography Workstation v3.01 by eluting over a gradient of potassium chloride (0.1–1.4 M) in 50 mM Tris•HCl buffer, pH 7.9; the enzyme generally eluted at 325–450 mM salt. Fractions bearing Y76L TruB that tested RNase-free were pooled, concentrated, and stored at –20 °C in 50 mM HEPES buffer, pH 7.5, containing ammonium chloride (100 mM), EDTA (1 mM), and glycerol (10%, v/v).

**Reaction between Y76L TruB and [F<sup>5</sup>U]TSL.** Y76L TruB (10 μM) was incubated at 37 °C with [F<sup>5</sup>U]TSL (50 μM) in TruB reaction buffer. For HPLC analysis of the RNA, an aliquot (10 μL) of the reaction mixture was diluted into S1 nuclease digestion buffer (90 μL), which is 30 mM sodium acetate buffer, pH 4.6, containing sodium chloride (50 mM), zinc chloride (10 mM), and glycerol (5%, v/v). S1 nuclease (0.5 μL, 50 U) was added, and the mixture was incubated for 1 h at 37 °C and then at 94 °C for 5 min followed by cooling on ice for 5 min. Subsequently, a fresh aliquot of S1 nuclease (1 μL, 100 U) and alkaline phosphatase (3 μL, 3 U) were added, and the mixture was incubated for 3 h at 37 °C. The digestion mixture was then analyzed over a ZORBAX SB-C18 analytical column (Agilent Technologies) connected to Beckman Coulter System Gold HPLC (Indianapolis, IN) equipped with a Model 168 programmable diode array detector module.

**Deuterium wash-in.** Deuterated reaction buffers were prepared by three cycles of lyophilization of standard reaction buffer to dryness and redissolution in D<sub>2</sub>O (>99%). All exchangeable protons in stem-loop RNAs were replaced with deuterium by three cycles of dissolution and lyophilization in D<sub>2</sub>O (>99%). RluA (10 μM) was mixed with ASL (100 μM) or RluA (110 μM) was mixed with [F<sup>5</sup>U]ASL (100 μM) and incubated for 3 h at 37 °C. The reaction mixture was then heated to 94 °C for 5 min, cooled on ice for 5 min, centrifuged (18,000g,

5 min) and spun to pellet the protein, which was discarded. Residual protein was extracted from the supernatant with 1:1 phenol/chloroform, and the RNA was precipitated with ethanol and air-dried. The RNA was redissolved in S1 nuclease digestion buffer (100  $\mu$ L), and digested to nucleosides by the combination of S1 nuclease ( $2 \times 5 \mu$ L with heat denaturation in between, 500 U each addition) and alkaline phosphatase (5  $\mu$ L, 5 U). After the complete digestion was confirmed by analytical HPLC,  $F^5U^*$  was isolated by preparative reverse phase HPLC over an ultrasphere•C18 column (5  $\mu$ M,  $10 \times 250$  mm; Beckman-Coulter, Fullerton, CA), eluting with a gradient of acetonitrile in water using the method described elsewhere<sup>10</sup> but with a flow rate of 3 mL/min. The fractions containing  $\Psi$  were combined and taken to dryness *in vacuo*, and  $\Psi$  was redissolved in 10% aqueous methanol/formic acid (98:2 v/v). The fractions containing  $F^5U^*$  were treated similarly, but redissolution was accomplished with aqueous methanol (10% v/v). For the experiments with Y76L TruB,  $[F^5U]TSL$  (50  $\mu$ M) in deuterated standard reaction buffer (146.5  $\mu$ L) was incubated for 5 min at 37 °C before the reaction was started by the addition of Y76L TruB (10  $\mu$ M, 3.5  $\mu$ L), which resulted in a final deuterium content of 96.6%. After 4 h at 37 °C, the reaction was worked up as described for the reactions with RluA and  $[F^5U]ASL$ . In all cases, control reactions were run identically in unlabeled reaction buffer (150  $\mu$ L) followed by the same work up and analysis as described for the reactions run in deuterated buffer.

High resolution mass spectrometry of the products was run ( $F^5U^*$  in negative mode and  $\Psi$  in positive mode) on a Thermo Finnigan (Bremen, Germany) linear trap quadrupole Fourier transform (LTQ-FT) mass spectrometer equipped with a Triversa Nanomate (Ithaca, NY) direct infusion nano-electrospray ionization (nESI) source. Data was analyzed using Xcalibur® software (Waltham, MA). For the labeled reaction (96.66%  $D_2O$ ), the isotopic contributions from each element ( $^2H$ ,  $^{13}C$ ,  $^{15}N$ ,  $^{18}O$ , etc.) in M+1 and M+2 peaks were calculated relative to the intensity of the monoisotopic peak, which was set to a value of 100%. The difference between the relative intensity value thus obtained for  $^2H$  and the relative intensity of the monoisotopic peak from the unlabeled reaction was then adjusted by the isotopic composition of the labeled buffer to obtain the percentage of deuterium wash-in.

**Enzymes for the synthesis of  $[2'-^2H]UTP$ .** The plasmid (pET22-HT) bearing the ribokinase gene (*rbsK*) was generously provided by J. Williamson,<sup>12</sup> but it did not properly express ribokinase. DNA sequencing revealed an overhang after the stop codon and an inverted duplication at the 5'-end. To rectify these errors and introduce *NdeI* and *BamHI* restriction sites at the 5'- and 3'-ends, respectively, *rbsK* was amplified by PCR using the following primers: 5'-GCTCCTCATATGCAAAACGCAGGCAGCC-3' (forward) and 5'-GCTTCGGGATCCTCACCTCTGCCTGT-3' (reverse). The PCR product was digested with *NdeI* and *BamHI* and ligated into pET-15b (Novagen; Billerica, MA) opened with the same restriction enzymes to create pUL600 for the expression of ribokinase with an N-terminal His<sub>6</sub>-tag. The proper insertion of *rbsK* into the plasmid was verified by DNA sequencing. BLR(DE3) pLysS was transformed with pUL600, and ribokinase was overexpressed and purified over Ni-NTA resin (QIAGEN) according to the protocol used for RluA.<sup>10</sup> Purified fractions of ribokinase were tested for activity, pooled, concentrated, and dialyzed into 50 mM phosphate buffer, pH 7.5, containing sodium chloride (150 mM) and diluted with an equal volume of glycerol for storage at -20 °C until needed.

The plasmids encoding *Salmonella enterica* PRPP synthetase and *E. coli* UPRTase were generously provided by S. Van Lanen.<sup>13</sup> Both plasmids

were based on pET-30a(+) (Novagen) so that the encoded proteins are expressed with an N-terminal His<sub>6</sub>-tag. Following transformation of BLR(DE3) pLysS cells with these plasmids, PRPP synthetase and UPRTase were overexpressed and purified over Ni-NTA resin. Column fractions were assayed for activity, and enzyme-bearing fractions were pooled, concentrated, and stored at -20 °C in 50 mM sodium phosphate buffer, pH 7.5, containing sodium chloride (300 mM) and glycerol (50% v/v).

Ribokinase, PRPP synthetase, and UPRTase were assayed as previously reported,<sup>12,14</sup> and the specific activities of each enzyme were in agreement with the literature values (Table S5).<sup>14</sup> For the PRPP synthetase assay, the commercially obtained barium salt of ribose 5-phosphate (100 mM, 1 mL) was exchanged into its sodium form by passage over a column (2  $\times$  1 cm) of Dowex-50 (Na<sup>+</sup> form); the recovered ribose 5-phosphate was quantitated by measuring the released inorganic phosphate<sup>15</sup> after dephosphorylation with alkaline phosphatase.

**Synthesis of  $[2'-^2H]uridine$  triphosphate.** The method of Tolbert and Williamson for enzymatic synthesis of nucleoside triphosphates<sup>12</sup> was adapted to a smaller scale (400  $\mu$ mol) for  $[2'-^2H]UTP$  synthesis. D- $[2'-^2H]$ Ribose (60.7 mg, 400  $\mu$ mol) and uracil (44.8 mg, 400  $\mu$ mol) were dissolved in synthesis buffer (50 mL), which is 50 mM potassium phosphate buffer, pH 7.5, containing DTT (20 mM), kanamycin (0.1 mM), ATP (0.5 mM), ampicillin (5 mM), magnesium chloride (10 mM), and PEP (40 mM). The synthesis was initiated by the addition of ribokinase (50 U), PRPP synthetase (50 U), UPRTase (2 U), nucleoside monophosphate kinase (2 U), myokinase (37.5 U), and pyruvate kinase (75 U).<sup>16</sup> The reaction was monitored both by  $^{31}P$  NMR and an assay of pyruvate formation.<sup>12,16</sup> After 108 h, no further increase in the amount of  $2'-[^2H]UTP$  was detected by  $^{31}P$  NMR, and the reaction was judged to be essentially complete (>90%) by pyruvate production. The reaction mixture was filtered through an Amicon DIAFLO YM-10 membrane (10,000 MWCO) to remove enzymes, and purified by the method of Stambaugh and Wilson.<sup>17</sup> Activated charcoal (2 g) was added to the reaction mixture (~48 mL) to adsorb UTP; after nutation for 15 min at 4 °C, the charcoal was pelleted by centrifugation (8000g, 15 min). The supernatant was discarded after  $A_{260}$  revealed that the bulk of  $[2'-^2H]UTP$  (and ATP) was adsorbed to the charcoal. The charcoal was washed successively with ice-cold water (20 mL) and aqueous ethanol (20 mL; 2.5%, v/v) containing ammonium hydroxide (0.5%, v/v). Finally, the charcoal-bound  $[2'-^2H]UTP$  along with other "sticky" reaction components (primarily PEP and ATP) were eluted from the charcoal with aqueous ethanol (2  $\times$  30 mL; 50% v/v) containing ammonium hydroxide (0.5% v/v). The ethanolic elutions (60 mL) containing  $[2'-^2H]UTP$  were combined and filtered through a Steriflip® vacuum filter unit to remove residual charcoal. The pH was adjusted to 6.5 using acetic acid (1 M), and the solution was evaporated to dryness *in vacuo*, which yielded  $[2'-^2H]UTP$  as yellowish white powder (247  $\mu$ mol, 61% yield).

To remove PEP and ATP that co-eluted with  $[2'-^2H]UTP$ , the yellowish white powder was dissolved in 5 mM triethylammonium acetate buffer (1 mL), pH 7.0, and loaded onto a Bond Elut C8 SPE cartridge pre-equilibrated with the same buffer: elution was achieved with steps of aqueous acetonitrile (0, 5, 10, 25, and 50%, v/v).  $[2'-^2H]UTP$  eluted in the first fraction (0% acetonitrile), PEP in the second (5% acetonitrile), and ATP in the third (10% acetonitrile). The fractions containing  $[2'-^2H]UTP$  were detected by the characteristic absorbance of uridine at 260 nm. These fractions were combined, and reduced in volume *in vacuo* using a rotary evaporator. Triethylammonium acetate was removed by the repeated addition and removal of water and



isopropanol *in vacuo* with maintenance of pH ~8.0 by the addition of aqueous sodium hydroxide (1 M). The [2'-<sup>2</sup>H]UTP was recovered as a white powder and stored at -80 °C (165 μmol, 41% yield from ribose).

<sup>1</sup>H NMR (400 MHz; D<sub>2</sub>O) δ: 7.95 (H<sup>6</sup>, 1H, d, *J* = 8.4 Hz), 5.95 (H<sup>1'</sup>/H<sup>6</sup>, 2H, m), 4.31 (H<sup>3'</sup>, 1H, d, *J* = 5.0 Hz), 4.23 (H<sup>4'</sup>/H<sup>5'</sup>/H<sup>5''</sup>, 3H, broad m).

<sup>31</sup>P NMR (162 MHz; D<sub>2</sub>O) δ: -5.97 (γ, d, *J* = 18.7 Hz), -9.98 (α, d, *J* = 19.5 Hz), -21.20 Hz (β, overlapping dd, *J*<sub>apparent</sub> = 19.2 Hz).

***In vitro* transcription of TSL.** The partially double-stranded DNA template was prepared using commercially obtained oligonucleotides that had the following sequence: 5'-CTGTGGATCGAACACAGCT ATAGTGAGTCGTATTA-3' (where underlining denotes the template sequence for TSL) and 5'-TAATACGACTCACTATAGC-3'. The template was annealed by incubating the strands together (50 mM each in a volume of 100 μL) for 5 min at 65 °C followed by cooling on ice for 5 min. This template was added to the transcription mixture (10 mL), which is 40 mM Tris•HCl buffer, pH 8.1, containing rNTPs (4 mM each), GMP (8 mM), magnesium chloride (25 mM), spermidine (1 mM), DTT (5 mM), Triton X-100 (0.01%, v/v), Prime RNase Inhibitor (10 U), and inorganic pyrophosphatase (5 U). The *in vitro* transcription reaction was initiated by adding T7 RNA polymerase (25000 U) and incubated for 9 h at 37 °C.<sup>11</sup> Urea-PAGE analysis was used to monitor the reaction progress. Periodically, an aliquot (3 μL) of the reaction mixture was withdrawn and diluted with water (10 μL final volume); 2× RNA loading dye (10 μL) was added, and the sample was then heated for 5 min at 94 °C, cooled on ice for 5 min, and loaded on to a urea-PAGE gel (15%, 7M urea). The transcription products were visualized with SYBR® Gold nucleic acid stain.

After analysis showed no further accumulation of TSL, TURBO™ DNase (5 μL, 10 U) was added to the transcription reaction, which was incubated for an additional 15 min at 37 °C. Proteins were extracted from the reaction mixture with 1:1 phenol/chloroform. The crude RNA in the collected aqueous phase was precipitated with ethanol and pelleted by centrifugation (8000g, 30 min). The pelleted RNA was washed with aqueous ethanol (70%, v/v), air dried, and dissolved in 10 mM Tris•HCl buffer, pH 7.5, containing EDTA (1 mM).

The transcript of interest (18-mer) was purified from the crude mixture by urea-PAGE electrophoresis (15%, 7M urea; 15 cm × 15 cm). The crude transcript (1 mL) was mixed with 2× RNA dye (1 mL), heated for 5 min at 94 °C, cooled on ice for 5 min, and loaded onto the gel. After being developed at 165 V for 6 h, the gel was removed, and the band of interest was located by UV-shadowing. RNA was extracted from the excised band either by electroelution using an Elutrap electrophoresis unit (GE Healthcare, Pittsburgh, PA) run at 200 V for 3 h, or by the crush and soak method.<sup>18</sup> RNA was ethanol-precipitated, pelleted by centrifugation (8000g, 30 min), and redissolved in RNase-free water. Purified TSL was divided into aliquots and stored at -20 °C. The labeled transcript was prepared identically to the unlabeled transcript, except that [2'-<sup>2</sup>H]UTP (4 mM) was substituted for UTP.

***In vitro* transcription of ASL.** The *in vitro* transcription of ASL with UTP and [2'-<sup>2</sup>H]UTP was identical to the synthesis of TSL except for the template, which was composed of 5'-GCGGATTTCATCCGC-TATACGTGAGTCGTATTA-3' (underlining indicates the complement to ASL) and 5'-TAATACGACTCACTATAGC-3'.

**Verification of transcripts.** An aliquot of the RNA oligonucleotide (10 μL, 80–100 μM) was diluted into RNase-free water (40 μL) to which RNase T1 (2 μL, 200 U) was added. After incubation for 1 h at 37 °C, alkaline phosphatase (5 μL, 5 U) was added to the digestion

mixture and incubated for an additional 3 h at 37 °C. An aliquot (3 μL) of the digest was then mixed with 3-HPA matrix solution (3 μL), which was 3-hydroxypicolinic acid (3-HPA; Fluka, Milwaukee, WI; 10 mg/mL) in 50% aqueous acetonitrile. The sample was spotted on a MALDI plate, air dried, and analyzed on a Voyager DE-Pro MALDI-TOF instrument or an API 4700 MALDI-TOF Mass spectrophotometer (PE Biosystems, Foster City, CA). Mass spectra were acquired either in positive or negative reflectron mode; calibration was achieved by a conventional 3-point method using a mixture of oligodeoxynucleotides as standards: TTTGCTT (2076.37 monoisotopic mass), T10 (2978.49), and T15 (4498.721). Data was analyzed with mMASS data analysis software, version 5.5.1.<sup>19</sup>

**Kinetic assays.** TruB and RluA were overexpressed, purified, and assayed as previously described.<sup>7,11</sup> For TruB, standard assay buffer is 50 mM HEPES buffer, pH 7.5, containing ammonium chloride (100 mM), EDTA (1 mM), and DTT (5 mM). TSL (1–10 μM) was pre-incubated in standard reaction buffer (400–2600 μL) for 3 min at 37 °C before reactions were initiated by the addition of a small volume (<2 μL) of TruB (to 10 nM). Aliquots (75–650 μL) were removed at various time intervals and quenched into pre-heated (100 °C) tubes containing 10× S1 nuclease digestion buffer (one tenth the aliquot volume), which is 300 mM sodium acetate buffer, pH 4.6, containing sodium chloride (500 mM), zinc chloride (100 mM), and glycerol (50%, v/v). After 5 min in a boiling water bath, the tubes were cooled on ice for 5 min. S1 nuclease (0.5 μL, 50 U) was added, and the mixture was incubated for 1 h at 37 °C; the digest was then incubated for 5 min at 94 °C followed by incubation on ice for 5 min. Another aliquot of S1 nuclease (1 μL, 100 U) and alkaline phosphatase (3 μL, 3 U) were added, and the mixture was incubated for 3 h at 37 °C. The digest was then passed through a Corning Costar™ spin filter (0.22 μm), and analyzed over a ZORBAX SB-C18 analytical column (Agilent Technologies) connected to Beckman Coulter System Gold HPLC (Indianapolis, IN) equipped with a Model 168 programmable diode array detector module.

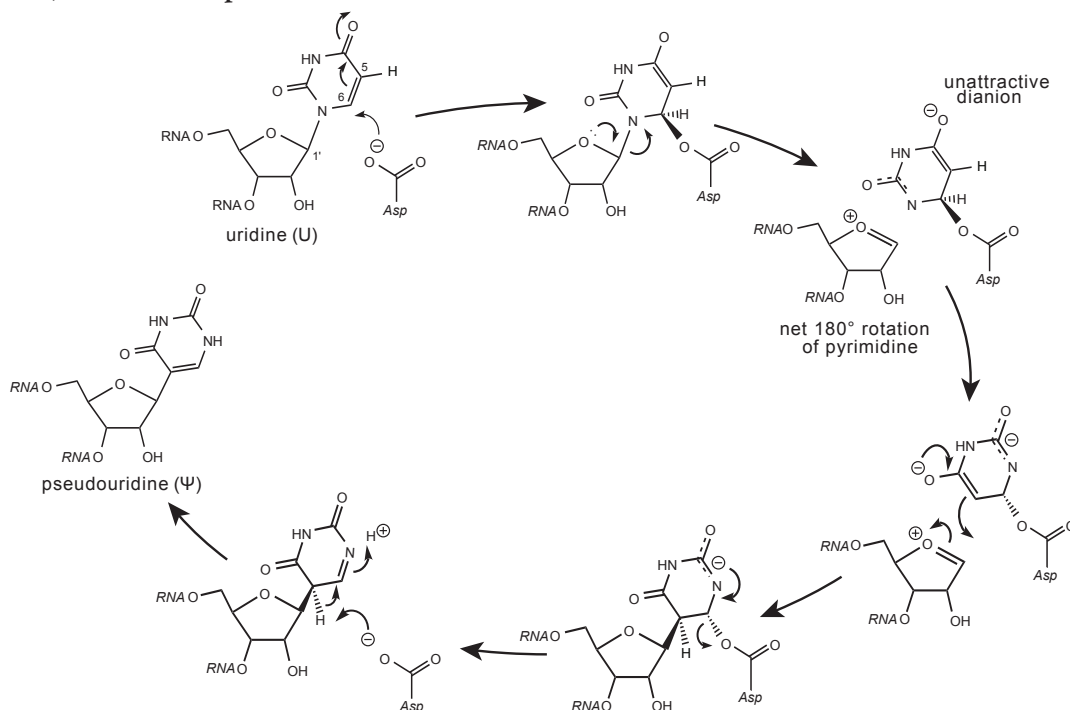
For RluA, the previously reported assay procedure<sup>7</sup> was modified because, unlike with chemically synthesized ASL, the *in vitro*-transcribed substrate ASL (with a reversed base pair and a 5'-phosphate) was not readily separable from its product (ASL with Ψ instead of U at the isomerized position). Similar to the TruB assay, the 17-mer ASL was digested to its component nucleosides and analyzed by HPLC to quantitate Ψ. The assay mixtures (450–2400 μL) were standard reaction buffer containing ASL (1–10 μM). After pre-incubation for 3 min at 37 °C, reactions were initiated by the addition of a small volume (<2 μL) of RluA (to 10 nM). Aliquots (100–600 μL) were removed at various time intervals and quenched and analyzed as described above for TSL.

## Mechanisms

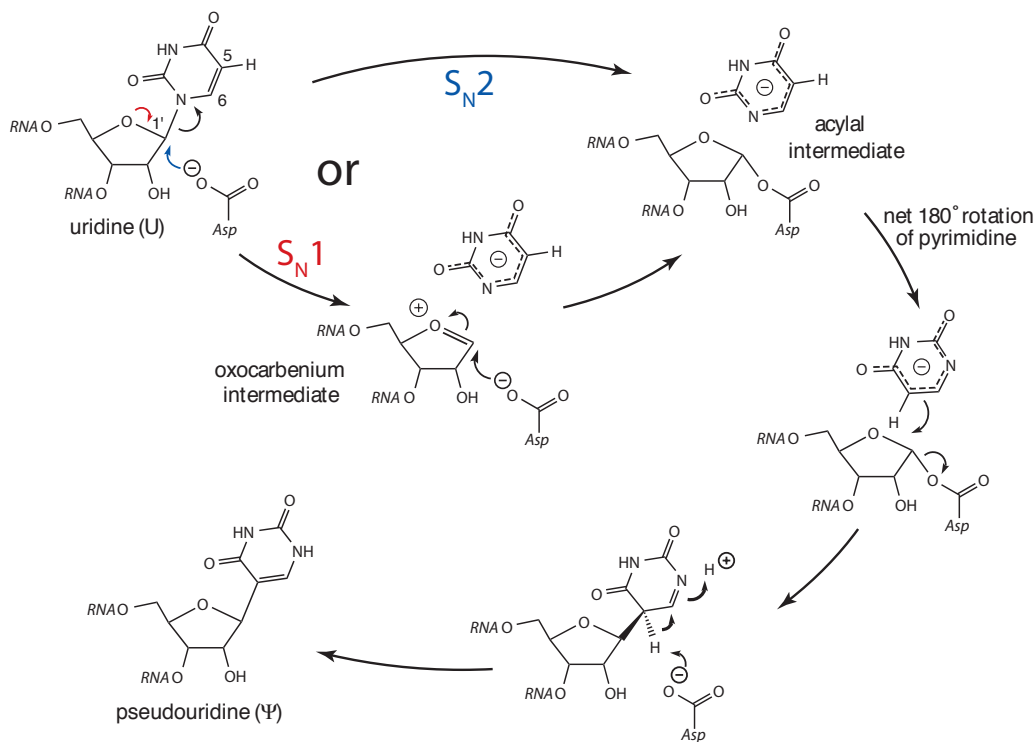
Three mechanisms have been proposed for the  $\Psi$  syntheses.<sup>20</sup> The “Michael mechanism” (Scheme S1) involves a Michael addition of the essential Asp by its nucleophilic attack at C6 of the pyrimidine ring to form an adduct.<sup>21,22</sup> The “acyl mechanism” (Scheme S2) instead involves the essential Asp nucleophilically attacking at C1' to form an acylal intermediate.<sup>23</sup> With [ $F^5U$ ]RNA, neither mechanism can pro-

ceed through the final step to give  $\Psi$  because the proton ( $H^5$ ) to be removed is replaced with fluorine. Scheme S3 is the acylal mechanism recast to emphasize features that can account for the observed arabino product of  $F^5U$ ; the reaction manifold (boxed in the figure) leading to the epimerized product is made possible by the increased lifetime of detached fluorouracilate ion relative to detached uracilate anion.<sup>8</sup>

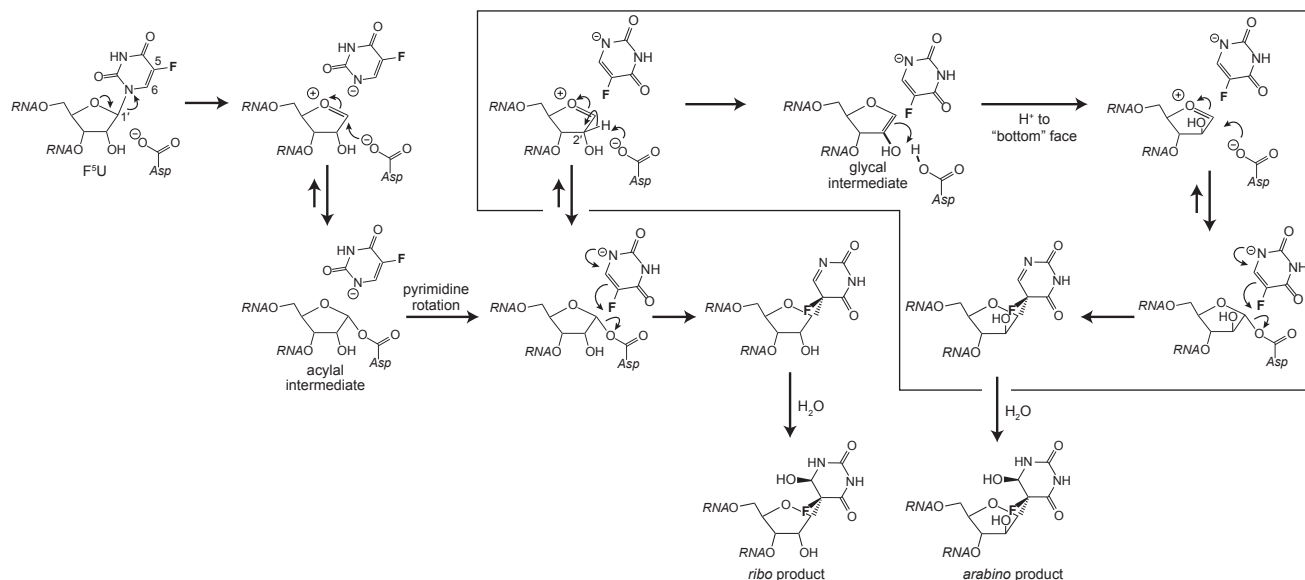
**Scheme S1.** The “Michael mechanism” involves the attack of the essential Asp at the pyrimidine ring (a Michael addition). With  $F^5U$ ,  $H^5$  is replaced with F, and the last step of the mechanism cannot occur.



**Scheme S2.** The “acyl mechanism” involves the attack of the essential Asp at the ribose ring to form an acylal intermediate. With  $F^5U$ ,  $H^5$  is replaced with F, and the last step of the mechanism cannot occur.



**Scheme S3. The acylal mechanism recast to account for the formation of the *arabino* product of F<sup>5</sup>U by the boxed reaction manifold.**

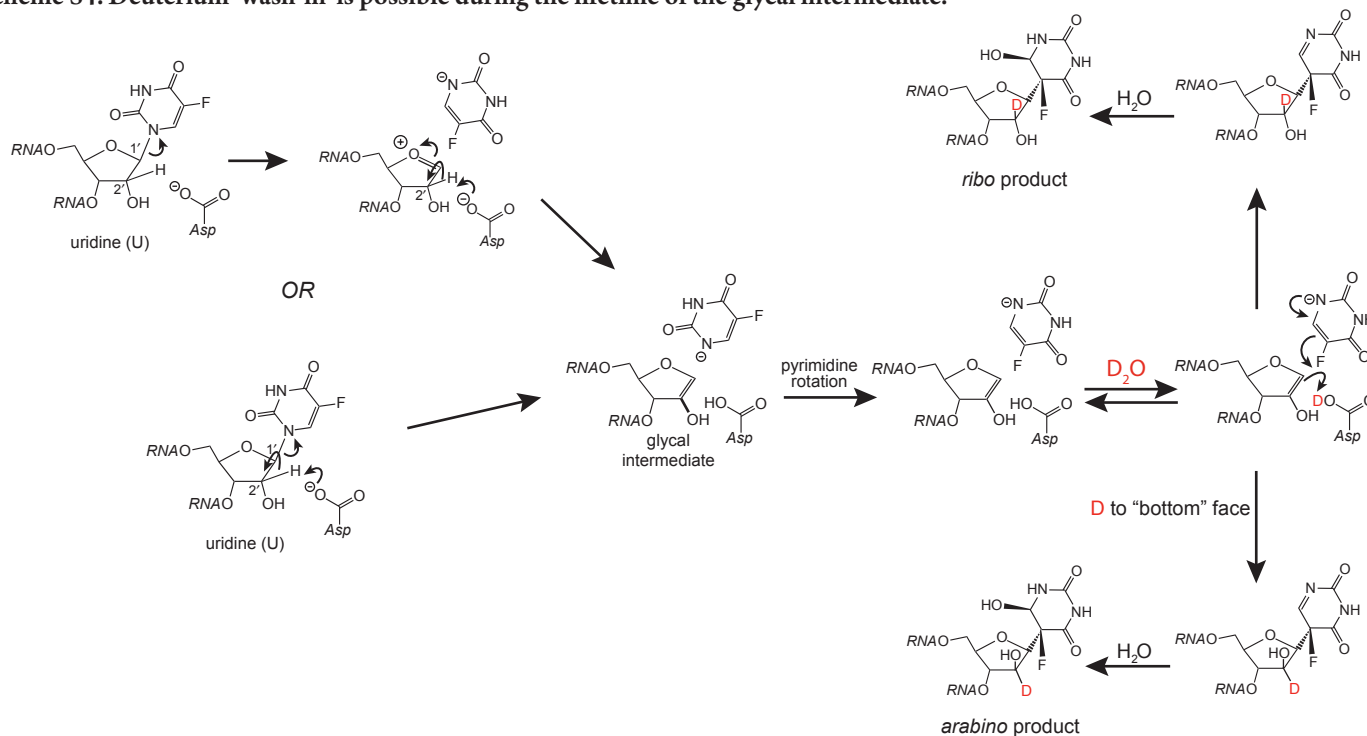


### Deuterium wash-in studies

**RluA.** If the handling of F<sup>5</sup>U by  $\Psi$  synthases proceeds through a glycol intermediate and the essential Asp acts as a base to deprotonate C2', then the removed proton should reside temporarily on the essential Asp, where it may be prone to exchange with the solvent protons (Scheme S4). An observed deuterium “wash-in” would thus provide evidence for a glycol intermediate along the reaction pathway. When TruB was incubated in deuterated buffer with RNA containing U or F<sup>5</sup>U, no deuterium wash-in was observed.<sup>8</sup> The same experiment was run with RluA, which revealed no deuterium incorporation into  $\Psi$  (Figure S1A and Table S1) or the products of F<sup>5</sup>U (F<sup>5</sup>U\*; Figure S1B and Table S2), which are isolated as dinucleotides because of the inability of S1 nuclease to cleave after non-planar bases.

**Y76L TruB.** The wash-in studies are contingent upon access of solvent to the active site, so the lack of wash-in remains consistent with a glycol intermediate since the essential Asp may remain occluded from the solvent on the timescale of the conversion of U or F<sup>5</sup>U. To enhance the opportunity for wash-in, an active mutant of TruB or RluA with a more spacious active site was sought. A tyrosine is conserved among five of the six families of  $\Psi$  synthases (the TruD family has a Phe<sup>24</sup>), and several previously described variants of TruB at this position (Tyr-76)<sup>25</sup> were investigated as candidates for further wash-in studies. Y76L TruB was generated *in silico*<sup>2</sup> and energy-minimized.<sup>1</sup> Comparison of the *in silico* structure of Y76L TruB and the cocrystal structure<sup>26</sup> of wild-type TruB and [F<sup>5</sup>U]RNA revealed a comparatively spacious

**Scheme S4. Deuterium ‘wash-in’ is possible during the lifetime of the glycol intermediate.**



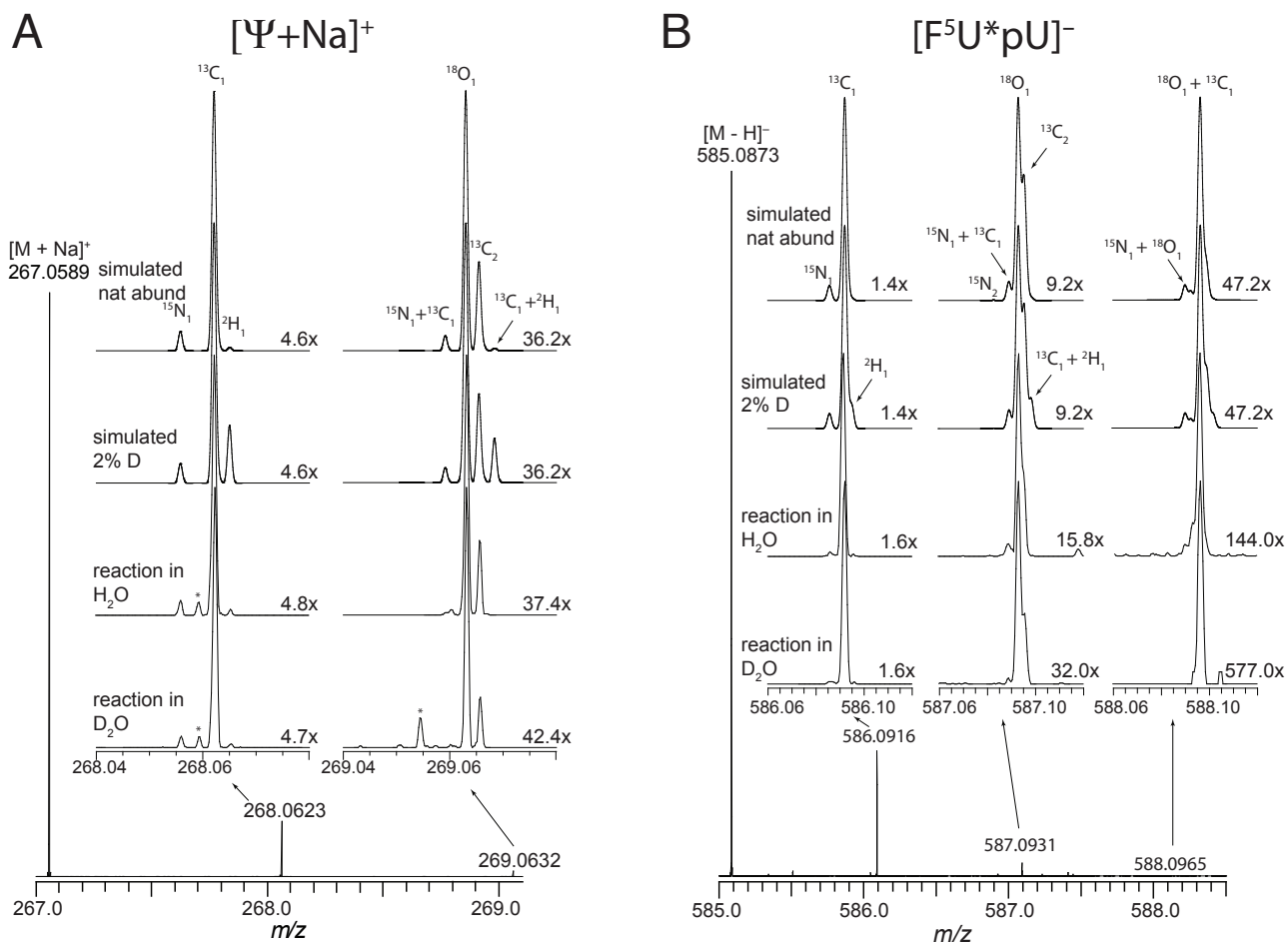


**Figure S1.** High resolution mass spectra of the products generated by RluA in deuterated buffer. (A)  $\Psi$  from the reaction of U in ASL (B) Products from the reaction of  $\text{F}^5\text{U}$  in  $[\text{F}^5\text{U}]\text{ASL}$  (the rearranged and hydrated  $\text{F}^5\text{U}$  products are isolated as dinucleotides with the U that follows  $\text{F}^5\text{U}$ ; see text for details). The insets are close-up views of the  $M+1$  and  $M+2$  ion clusters. The spectra for the products obtained from the reaction run in unlabeled buffer ( $\text{H}_2\text{O}$ ) and deuterated buffer ( $\text{D}_2\text{O}$ ) are presented along with the simulated spectra for natural abundance (simulated nat abund) and for 2% non-exchangeable deuterium (simulated 2% D). \*, unidentified peaks absent in the control mass spectrum of solvent.

**Table S1.** High resolution mass spectrometry data (positive mode) for pseudouridine ( $\text{C}_9\text{H}_{12}\text{N}_2\text{O}_6$ ) from the RluA-catalyzed reaction of ASL in unlabeled and deuterated buffer.

Peak	Description	Predicted for $\text{C}_9\text{H}_{12}\text{N}_2\text{O}_6^a$		Observed			
		$m/z$	RA (%) <sup>b</sup>	unlabeled buffer		deuterated buffer	
		$m/z$	RA (%) <sup>b</sup>	$m/z$	RA (%) <sup>b</sup>	$m/z$	RA (%) <sup>b</sup>
monoisotopic	$[\text{M}+\text{Na}]^+$	267.0588	100.0	267.0589	100.0	267.0589	100.0
$^{13}\text{C}_1$ ion cluster	$^{15}\text{N}_1$	268.0558	0.7	268.0560	0.5	268.0560	0.4
	$^{13}\text{C}_1$	268.0621	9.7	268.0623	9.3	268.0623	9.5
	$^2\text{H}_1$	268.0650	0.1	268.0650	0.2	268.0653	0.1
$^{13}\text{C}_2$ ion cluster	$^{18}\text{O}_1$	269.0631	1.2	269.0632	1.2	269.0632	1.0
	$^{13}\text{C}_2$	269.0655	0.4	269.0656	0.3	269.0656	0.2

<sup>a</sup>Predicted from natural abundance

<sup>b</sup>Relative abundance



**Table S2.** High resolution mass spectrometry data (negative mode) for the dinucleotide product ( $F^5U^*pU$ ;  $C_{18}H_{24}FN_4O_{15}P$ ) obtained from the reaction of RluA and  $[F^5U]$ ASL in unlabeled and deuterated buffer.

Peak	Description	Predicted for $C_{18}H_{24}FN_4O_{15}P^a$		Observed			
		$m/z$	RA (%) <sup>b</sup>	unlabeled buffer $m/z$	unlabeled buffer RA (%) <sup>b</sup>	deuterated buffer $m/z$	deuterated buffer RA (%) <sup>b</sup>
monoisotopic	$[M-H]^-$	585.0887	100.0	585.0873	100.0	585.0878	100.0
$^{13}C_1$ ion cluster	$^{15}N_1$	586.0857	1.5	586.0859	0.4	586.0859	0.2
	$^{13}C_1/^{2}H_1$	586.0921	19.8	586.0916	17.9	586.0921	17.5
$^{13}C_2$ ion cluster	$^{15}N_1 + ^{13}C_1$	587.0892	0.3	ND <sup>c</sup>	—	ND	—
	$^{18}O_1$	587.0930	3.1	587.0931	2.0	587.0931	0.9
	$^{13}C_2$	587.0954	1.9	587.0957	0.7	587.0957	0.3
$^{13}C_3$ ion cluster	$^{15}N_1 + ^{18}O_1$	588.0904	<0.1	ND	—	ND	—
	$^{18}O_1 + ^{13}C_2$	588.0965	0.6	588.0965	0.2	588.0965	<0.1

<sup>a</sup>Predicted from natural abundance

<sup>b</sup>Relative abundance

<sup>c</sup>Not detected

active site—and thus perhaps greater solvent accessibility—in the variant, primarily due to the lack of steric hindrance associated with the phenyl ring of Tyr-76 (Figure S2). The positioning of  $F^5U$  within the active site of the Y76L TruB mutant was held fixed due to software limitations that allow energy minimization of the protein itself but not bound molecules such as the RNA substrate.

Despite the modeling limitations, the predictions were judged sufficiently encouraging to proceed, so the Y76L mutation was introduced into the *truB* gene in pY55, the pET15b-based vector for overexpression of the N-terminally His<sub>6</sub>-tagged TruB,<sup>10,11</sup> to create pUL323. The identity of overexpressed Y76L TruB (Figure S3) was confirmed by digestion with chymotrypsin or pepsin and MALDI-TOF mass spec-

trometry of the resulting peptides (data not shown). Y76L TruB lost over half its activity within one week when stored under the conditions used for the wild-type TruB.<sup>11</sup> This instability was successfully addressed by storage at  $-20^\circ\text{C}$  in 50 mM HEPES buffer, pH 7.5, containing ammonium chloride (100 mM), EDTA (1 mM), and glycerol (10%, v/v). Under these conditions, the stability of Y76L TruB improved, with <15% loss of activity after one month.

Similar to wild-type TruB,<sup>27</sup> no adduct was observed on SDS-PAGE gels between Y76L TruB and  $[F^5U]$ RNA (data not shown). Y76L TruB handles  $F^5U$  in RNA ~600-fold more slowly than wild-type TruB (Table S3), but sluggish catalysis could be propitious for wash-in because the time that the proton putatively resides on the essential Asp

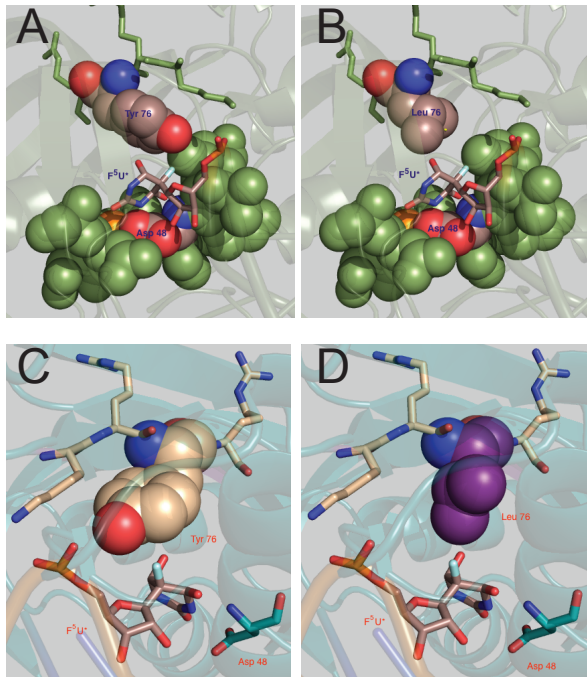


**Figure S2.** Y76L TruB has a more spacious active site than wild-type TruB. Active site amino acid residues other than Leu-76/Tyr-76 are in green. (A) Wild-type TruB. (B) *In silico*-generated Y76L TruB. The orientation of the pyrimidine ring relative to residue 76 also differs. (C) Wild-type TruB (D) Y76L TruB

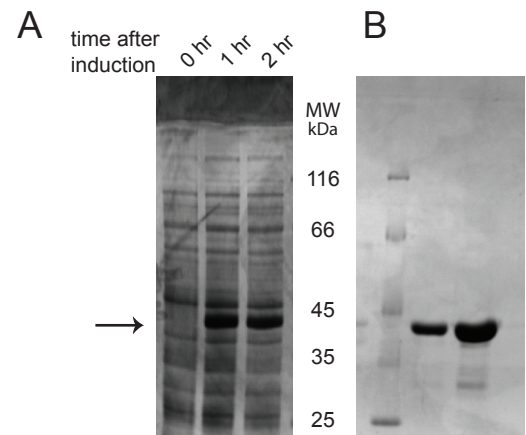


**Figure S3.** SDS-PAGE analysis of Y76L TruB. (A) Overexpression. (B) The purified enzyme at two loading levels. The arrow indicates Y76L TruB (36.8 kDa); MW, molecular weight marker.

**Table S3.** Time course for the formation of  $[F^5U^*]$ TSL by the action of Y76L TruB on  $[F^5U]$ TSL (50  $\mu\text{M}$ ).

Y76L TruB, $\mu\text{M}$	time, h	$[F^5U^*]$ TSL, $\mu\text{M}$
10	3	18
10	6	21
10	12	25
5	3	10

may increase, depending on which reaction step(s) were slowed. As previously reported,<sup>25</sup> HPLC analysis of the constituent nucleosides of product RNA (obtained by digestion with S1 nuclease and alkaline phosphatase) showed a single peak for F<sup>5</sup>U\* that displayed an identical retention time to that of the major (*ribo*) product of F<sup>5</sup>U from the action of wild-type TruB; this assignment was confirmed by co-injection of the RNA digests from reactions with wild-type and Y76L TruB, which displayed the expected increase in the area of the peak accounting for the major (*ribo*) product (Figure S4). The altered behavior of Y76L TruB towards [F<sup>5</sup>U]RNA can be ascribed to the change in relative positioning of F<sup>5</sup>U within the active site so that the essential Asp can no longer reach the “bottom” face of the glycal for reprotonation at C2'. This rationale could not easily be examined further because the employed software<sup>8</sup> does not allow energy minimization of protein ligands (such as the bound RNA).

To quantify the ability of Y76L TruB to turn over the stem-loop RNA containing F<sup>5</sup>U ([F<sup>5</sup>U]TSL), the variant was incubated with an ex-

cess of [F<sup>5</sup>U]TSL (5- to 10-fold), and aliquots were withdrawn at regular intervals for digestion to individual nucleosides and analysis by HPLC. Wild-type TruB (200 nM) completely turns over [F<sup>5</sup>U]TSL (20 μM) into [F<sup>5</sup>U\*]TSL within 3 h,<sup>27</sup> but Y76L TruB (5–10 μM) achieved only ~2.5 turnovers after 12 h (~600-fold decrease in activity). When Y76L TruB (2.5 μM) was pre-incubated with [F<sup>5</sup>U\*]TSL (5 μM) prior to incubation with [F<sup>5</sup>U]TSL (50 μM), a further reduction in initial rate was observed (Figure S5), evocative of a binding competition between [F<sup>5</sup>U]TSL and [F<sup>5</sup>U\*]TSL.

Mass spectra were obtained for F<sup>5</sup>U\*pC resulting from the action of Y76L TruB in either unlabeled or deuterated standard reaction buffer. An encouraging level of deuterium wash-in (4.45%) was observed in a preliminary run, but replication showed insubstantial deuterium incorporation (0.52% and 0.92%) into F<sup>5</sup>U\*pC (Table S4).

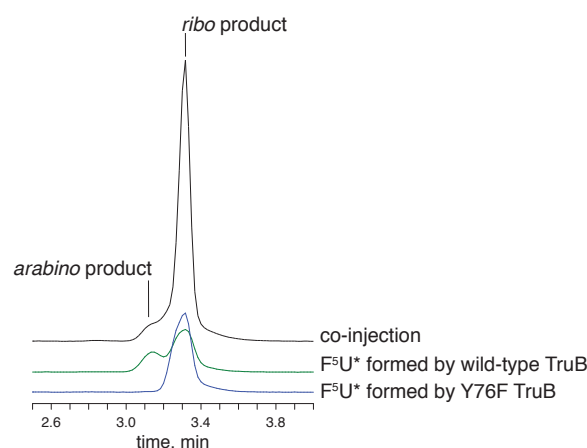


**Figure S4.** HPLC analysis of the products of F<sup>5</sup>U from the action of TruB. Wild-type TruB (green trace) generates two partially resolved products (*ribo* and *arabino*), but Y76L TruB (blue trace) generates only one of them (*ribo*). Co-injection (black) results in a stoichiometric increase in the integration of the *ribo* product.

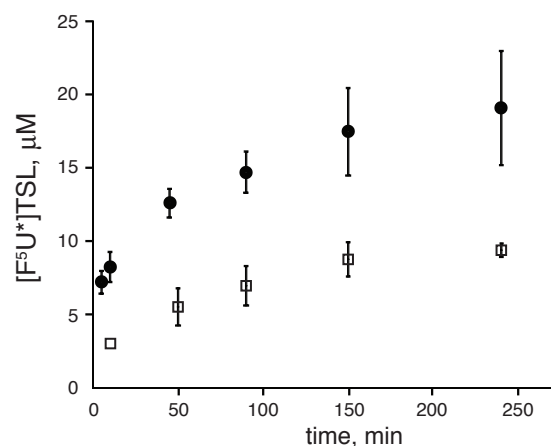


**Figure S5.** Inhibition of Y76L TruB by [F<sup>5</sup>U\*]TSL. Formation of [F<sup>5</sup>U\*]TSL by Y76L TruB (10 μM) with (□) and without (●) pre-incubation with [F<sup>5</sup>U\*]TSL (20 μM) prior to addition of [F<sup>5</sup>U]TSL (50 μM). The plotted values for the reaction with pre-incubation are adjusted by subtraction of the [F<sup>5</sup>U\*]TSL (20 μM) originally present.



**Table S4.** High resolution mass spectrometry data (negative mode) for the dinucleotide product ( $F^5U^*pC$ ;  $C_{18}H_{25}FN_5O_{14}P$ ) obtained from the reaction of RluA and  $[F^5U]$ ASL in unlabeled and deuterated buffer.

Peak	Description	Predicted for		Observed			
		$C_{18}H_{25}FN_5O_{14}P^a$		unlabeled buffer		deuterated buffer	
		$m/z$	RA (%) <sup>b</sup>	$m/z$	RA (%) <sup>b</sup>	$m/z$	RA (%) <sup>b</sup>
Trial A							
monoisotopic	$[M-H]^-$	584.105	100	584.107	100	584.105	100
$^{13}C_1$ ion cluster	$^{15}N_1$	585.101	1.85	585.103	1.79	585.104	0.50
	$^{13}C_1$	585.108	19.84	585.111	17.54	585.110	12.35
	$^2H_1$	585.111	0.48	585.113	ND <sup>c</sup>	585.114	0.52
$^{13}C_2$ ion cluster	$^{15}N_2$	586.105	0.37	586.106	0.04	586.107	0.05
	$^{18}O_1$	586.109	2.98	586.111	0.10	586.112	1.18
	$^{13}C_2$	586.111	1.94	586.112	ND	586.114	0.55
	$^{13}C_2 + ^{12}H_1$	586.115	0.06	586.117	0.04	568.114	0.02
Trial B							
monoisotopic	$[M-H]^-$	584.105	100	584.107	100	584.107	100
$^{13}C_1$ ion cluster	$^{15}N_1$	585.101	1.85	585.103	1.79	585.105	0.81
	$^{13}C_1$	585.108	19.84	585.111	17.54	585.110	14.62
	$^2H_1$	585.111	0.48	585.113	0.05	585.113	0.97
$^{13}C_2$ ion cluster	$^{15}N_2$	586.105	0.37	586.106	0.04	586.108	0.11
	$^{18}O_1$	586.109	2.98	586.111	0.10	586.112	1.19
	$^{13}C_2$	586.111	1.94	586.112	ND	586.114	0.59
	$^{13}C_2 + ^{12}H_1$	586.115	0.06	586.117	ND	586.117	0.03

<sup>a</sup>Predicted from natural abundance

<sup>b</sup>Relative abundance

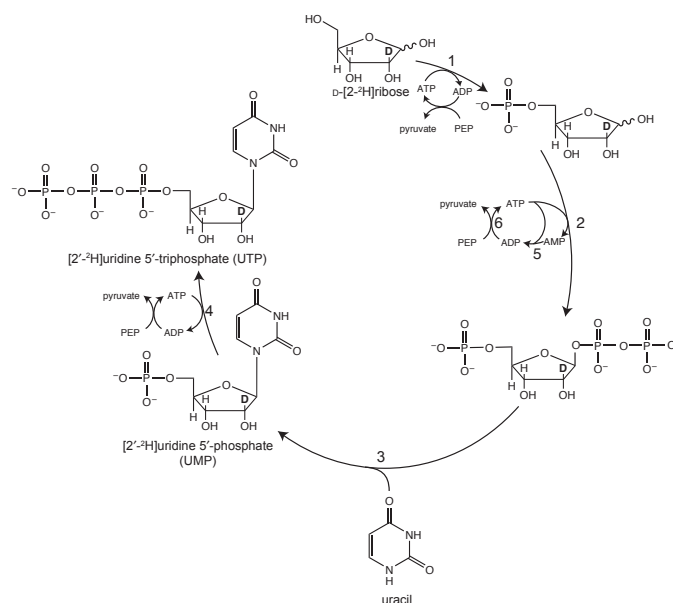
<sup>c</sup>Not detected

## Deuterium Kinetic Isotope Effect Studies

**Overview of substrate preparation.** The proposed glycol mechanism proceeds with deprotonation/reprotonation at C2', and if either of those steps (or both) are partially rate limiting, a kinetic isotope effect (KIE) is expected for a substrate deuterated at C2'. Substrates required for these studies (with U and  $[2\text{'-}^2H]U$ ) were prepared by *in vitro* transcription<sup>28</sup> with  $[2\text{'-}^2H]UTP$  synthesized enzymatically by the method of Tolbert and Williamson<sup>12</sup> with slight modification (Scheme S5). Glyceraldehyde 3-phosphate was substituted with phosphoenolpyruvate (PEP) to reduce the steps required for the *in situ* regeneration of ATP, which was achieved at the expense of PEP using pyruvate kinase and myokinase. To avoid buildup of ADP, the activity of myokinase was maintained at half the level of pyruvate kinase. Enzymes not commercially available were overexpressed.

**Enzyme overexpression.** The plasmid encoding ribokinase (pET-22HT)<sup>12</sup> showed poor levels of overexpression, and the specific activity of overexpressed enzyme was quite low in comparison to the literature values (Table S5).<sup>14</sup> DNA sequencing revealed insertions at both ends of the ribokinase gene (*rbsK*). To eliminate these insertions, *rbsK* was amplified by PCR using primers that restored the native gene and introduced *NdeI* and *BamHI* restriction sites that were used to place *rbsK* in pET-15b. Use of this recombinant plasmid (pUL600) resulted in improved levels of expression for ribokinase of specific activity somewhat greater than literature values (Table S5). The overex-

**Scheme S5. Enzymatic synthesis of  $[2\text{'-}^2H]UTP$ .** ATP is regenerated *in situ* at the expense of PEP by pyruvate kinase and myokinase. 1, ribokinase; 2, PRPP synthetase; 3, UPRTase; 4, nucleoside monophosphate kinase; 5, myokinase; 6, pyruvate kinase.



pression of PRPP synthetase and UPRTase was uneventful, and the isolated enzymes displayed specific activities comparable to literature values (Table S5).

**[2'-<sup>2</sup>H]UTP.** [2'-<sup>2</sup>H]UTP was synthesized by enzymatic condensation of D-[2-<sup>2</sup>H]ribose and uracil (Scheme S5). The first step of this one pot synthesis involves phosphorylation of D-[2-<sup>2</sup>H]ribose by ribokinase. Phosphoribosylpyrophosphate (PRPP) synthetase then converts D-[2-<sup>2</sup>H]ribose 5-phosphate into [2-<sup>2</sup>H]PRPP, which in turn gets converted into [2'-<sup>2</sup>H]UMP by uracil phosphoribosyl transferase (UPRTase). [2'-<sup>2</sup>H]UMP is phosphorylated at the expense of ATP by nucleoside monophosphate kinase, which is further phosphorylated to [2'-<sup>2</sup>H]UTP by pyruvate kinase at the expense of PEP.

**Table S5.** Specific activities of enzymes used in the synthesis of [2'-<sup>2</sup>H]UTP.

enzyme	specific activity μmol min <sup>-1</sup> mg <sup>-1</sup>	reported specific activity <sup>a</sup> μmol min <sup>-1</sup> mg <sup>-1</sup>
ribokinase	0.2 ± 0.1 <sup>b</sup> 100 ± 13 <sup>c</sup>	36
PRPP synthetase	9.1 ± 1.3	11
URPTase	7.0 ± 0.6	15

<sup>a</sup>Values from reference 14

<sup>b</sup>Overexpressed from pET-22HT

<sup>c</sup>Overexpressed from pUL600

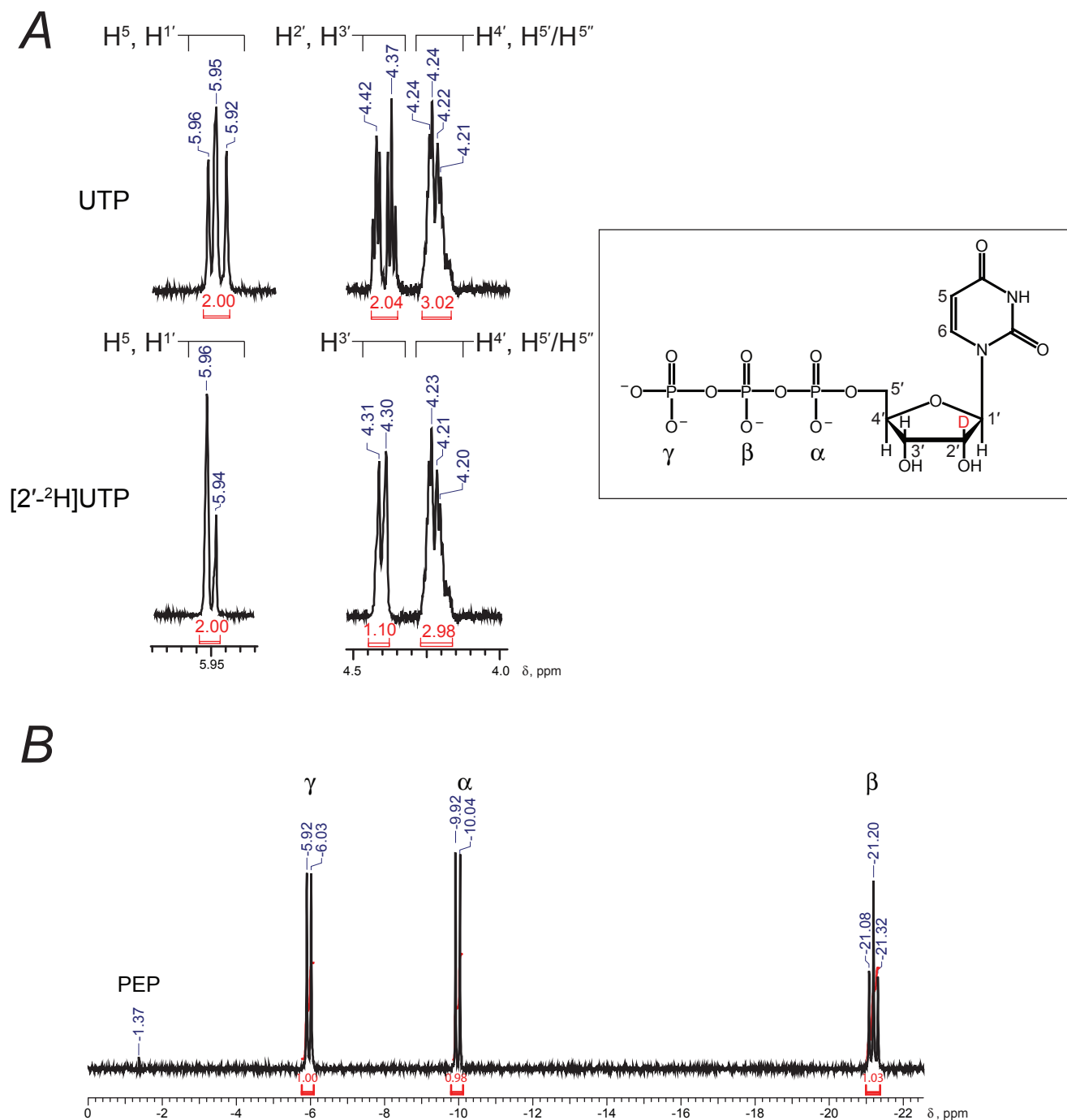


**Figure S6.** NMR characterization of [2'-<sup>2</sup>H]UTP (boxed structure). (A) Partial <sup>1</sup>H NMR spectrum showing the absence of H<sup>2'</sup> and the simplified splitting of H<sup>1'</sup> and H<sup>3'</sup> in the spectrum of the 2'-deuterated molecule (lower) relative to unlabeled (upper) UTP. (B) <sup>31</sup>P NMR spectrum.

The progress of  $[2\text{'-}^2\text{H}]\text{UTP}$  synthesis was monitored by  $^{31}\text{P}$  NMR and a coupled assay resting on the combined action of pyruvate kinase and lactate dehydrogenase. The labeled product was purified in three steps. First, enzymes were removed by ultrafiltration. Second, more than 90% of PEP, inorganic phosphate, and pyruvate were removed by the adsorption of  $[2\text{'-}^2\text{H}]\text{UTP}$  and ATP onto charcoal followed by rinsing steps and elution with aqueous ethanol. Third,  $[2\text{'-}^2\text{H}]\text{UTP}$  was freed of residual ATP and PEP by solid phase extraction over a Bond Elut C8 SPE cartridge.  $[2\text{'-}^2\text{H}]\text{UTP}$  (167  $\mu\text{mol}$ , 41% yield from D- $[2\text{'-}^2\text{H}]\text{ribose}$ ) was >95% pure as judged by NMR (Figure S6).

**In vitro transcription.** Unlabeled and labeled stem-loop RNA substrates for TruB and RluA were prepared by run-off *in vitro* transcription using T7 RNA polymerase.<sup>28</sup> The template and rNTP concentrations and reaction time were optimized because transcription efficiency is highly sensitive to these variables as well as the length of the transcript.<sup>29</sup> The transcription of these short stem-loops (17–19-mers) required a higher concentration of DNA template (0.5  $\mu\text{M}$ ) and a longer incubation (9 h) compared to the transcription of full length tRNA (a 76-mer).<sup>11</sup>

**TSL.** The canonical 17-mer RNA substrate for TruB<sup>6</sup> is the T-arm stem-loop (TSL) from *S. cerevisiae* tRNA<sup>Phe</sup>; it starts with a 5'-cytidine, but T7 RNA polymerase requires G as the initial nucleotide for efficient transcription. Therefore, two TSL transcripts of lengths 18 (5'-G added to canonical TSL) and a 19-mer (5'-GG added) were transcribed *in vitro* and obtained in comparable yields (9  $\mu\text{mol}$  for the 18-mer *versus* 11  $\mu\text{mol}$  for the 19-mer). When these transcripts (5  $\mu\text{M}$ ) were incubated with *E. coli* TruB (0.5  $\mu\text{M}$ ) in standard reaction buffer for 1 h at 37 °C, analysis of the digested nucleosides by reverse phase HPLC showed complete conversion for both transcripts, demonstrating their competence as substrates. With a shorter incubation time (1 min), the 18-mer (64.5%) showed greater conversion of U to  $\Psi$  than the 19-mer (52.0%), so the 18-mer RNA was chosen for large-scale transcription. After optimization of conditions, UTP and  $[2\text{'-}^2\text{H}]\text{UTP}$  were used in separate transcription reactions to generate unlabeled and labeled 18-mer TSL (Figure S7).

**ASL.** The canonical 17-mer substrate for RluA<sup>7</sup> is the anticodon stem-loop from *E. coli* tRNA<sup>Phe</sup> (ASL); it starts with a string of four Gs, but small-scale transcription revealed a “ladder” of transcription products rather than a single one (Figure S8A) due to the anomalous “slippage” experienced by T7 RNA polymerase when transcribing RNA beginning with a stretch of three or more Gs.<sup>29</sup> This issue was addressed by designing a DNA template that encodes ASL with a reversed (C:G) base pair at the second position (Figure S8B and S8C).

**Transcript sequence verification.** The sequences of unlabeled and labeled TSL and ASL transcripts were verified by digestion with RNase T1 and alkaline phosphatase followed by analysis with MALDI-TOF mass spectroscopy. The digestion products containing  $[2\text{'-}^2\text{H}]\text{U}$  showed a corresponding increase in the  $m/z$  value when compared to their unlabeled counterparts (Figures S9 and S10).

**Kinetic assays.** TruB was assayed under previously reported conditions.<sup>11</sup> The efficacy of the quench methodology was verified by analyzing time points for each assay immediately after addition of TruB to initiate the reaction: none of these initial time points showed any conversion of U to  $\Psi$ . Because intact substrate (TSL<sup>U</sup>) did not separate from intact product (TSL <sup>$\Psi$</sup> ), the product RNA was digested to individual nucleosides to quantify  $\Psi$  formation. Assays using the *in vitro* transcribed TSL and ASL revealed that they were efficient substrates and comparable to the purchased canonical TSL and ASL used in ear-

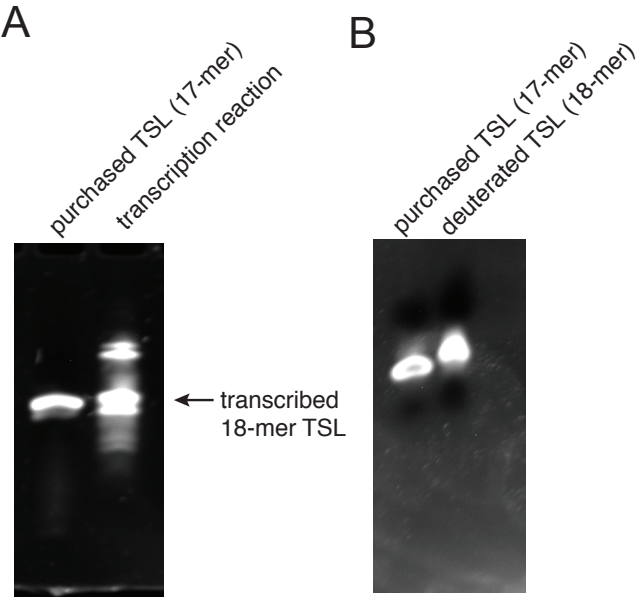


**Figure S7.** PAGE (15%, 7 M urea) analysis of *in vitro* transcribed TSL (18-mer). (A) Crude transcription reaction. (B) Purified deuterated TSL.

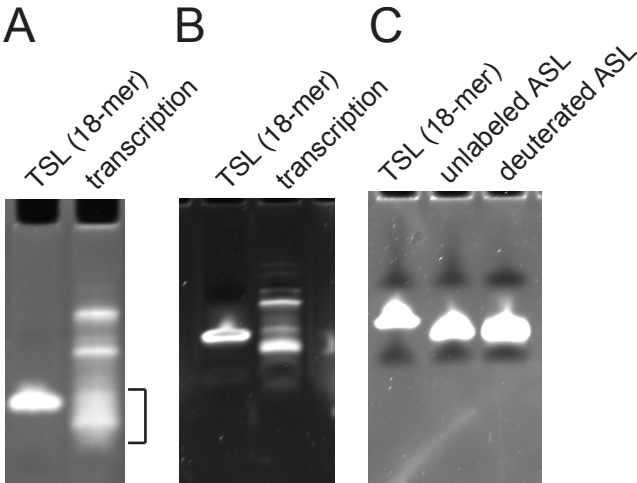


**Figure S8.** PAGE (15%, 7 M urea) analysis of *in vitro* transcribed ASL (17-mer). (A) Crude transcription reaction of canonical ASL showing initiation ‘slippage’ (indicated by the bracket). (B) Crude transcription reaction of ASL with the second base pair reversed. (C) Purified ASL transcripts.

**Table S6.** Comparison of kinetic parameters for TruB and RluA with synthesized and *in vitro* transcribed stem-loop substrates.

substrate	$k_{\text{cat}}$ s <sup>-1</sup>	$K_m$ $\mu\text{M}$
TruB with TSL		
synthesized <sup>a</sup>	0.24	0.8
<i>in vitro</i> transcript	0.34 ± 0.02	1.3 ± 0.3
RluA with ASL		
synthesized <sup>b</sup>	0.24	0.8
<i>in vitro</i> transcript	0.34 ± 0.02	1.3 ± 0.3

<sup>a</sup>Values from reference 6

<sup>b</sup>Values from reference 7

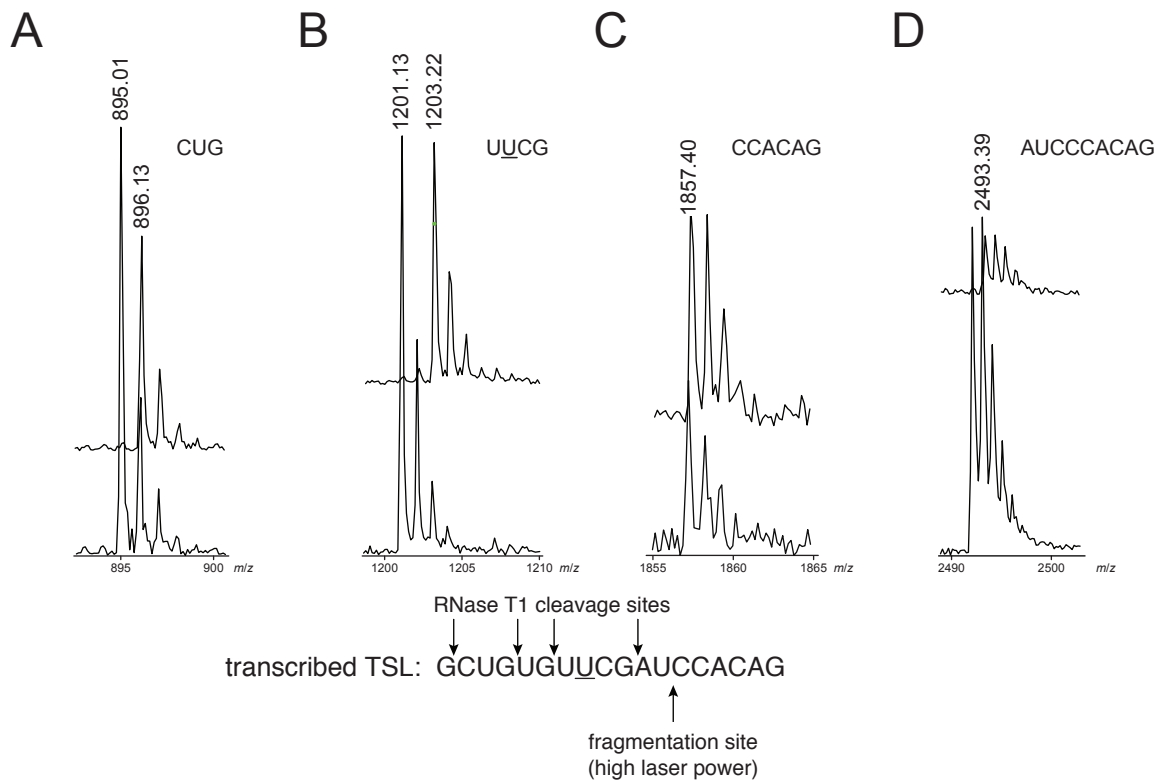


**Figure S9.** Partial MALDI-TOF mass spectra for the RNase T1 digests of unlabeled (lower trace) and deuterated (upper trace) transcribed TSL. (A) CUG ( $895.16 m/z_{pred}$ ). (B) UUCG ( $1201.19 m/z_{pred}$ ). (C) CCACAG ( $1857.33 m/z_{pred}$ ). (D) AUCCACAG ( $2492.40 m/z_{pred}$ ). Nucleotides and dinucleotides are not typically observed by MALDI MS under these conditions;  $m/z_{pred}$  is the predicted monoisotopic mass for the unlabeled oligonucleotide; the isomerized U is underlined.

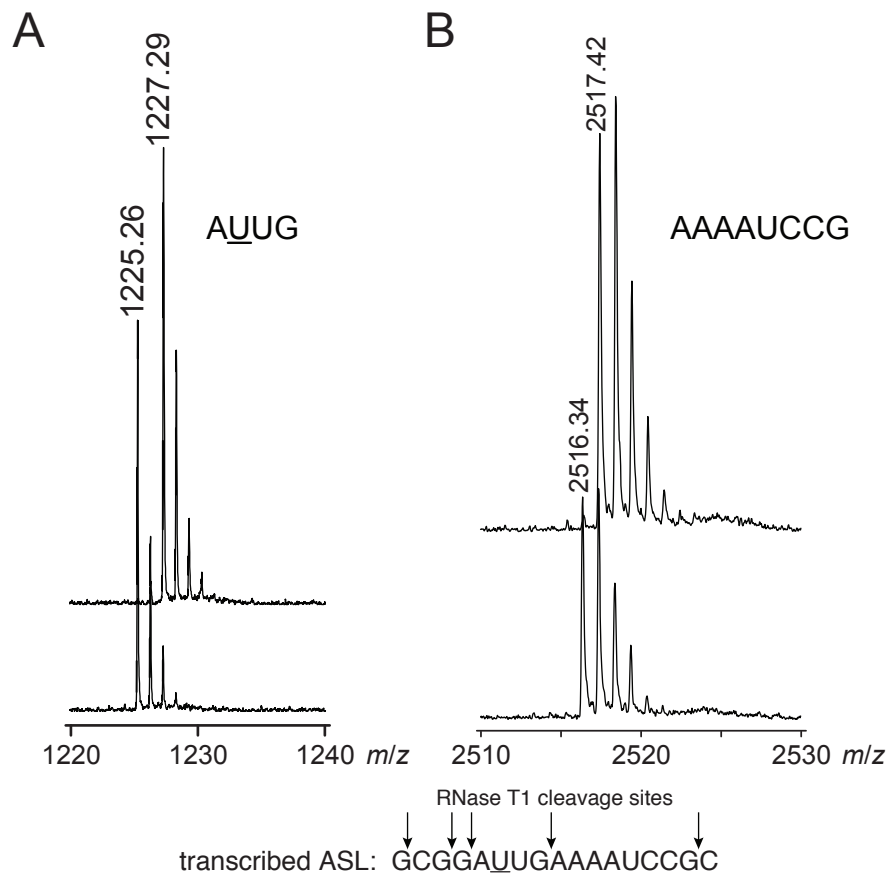


**Figure S10.** Partial MALDI-TOF mass spectra for the RNase T1 digests of unlabeled (lower trace) and deuterated (upper trace) transcribed ASL. (a) AUUG ( $1225.26 m/z_{pred}$ ). (b) AAAAUCCG ( $2516.42 m/z_{pred}$ ). Nucleotides and dinucleotides are not typically observed by MALDI MS under these conditions;  $m/z_{pred}$  is the predicted monoisotopic mass for the unlabeled oligonucleotide; the isomerized U is underlined.



lier studies (Table S6).<sup>6,7</sup> The assays for the labeled and unlabeled substrates were performed at variable substrate concentrations, and the initial velocity data was fit to Briggs-Haldane equation (Figure 2) to determine the values of  $k_{\text{cat}}$  and  $K_{\text{m}}$ , which revealed primary deuterium KIEs (Table 1) on both  $V_{\text{max}}$  (2.5) and  $V_{\text{max}}/K_{\text{m}}$  (3.6).

The assay for RluA was similar to that of TruB. The reaction quench methodology and the reverse phase HPLC-based quantification of

ASL<sup>‡</sup> were different from those previously reported<sup>7</sup> because the *in vitro* transcribed ASL<sup>U</sup> failed to separate from ASL<sup>‡</sup>. The assays for the labeled and unlabeled substrates were performed at varied substrate concentrations, and the initial velocity data was fit to the Briggs-Haldane equation (Figure 2). The  $k_{\text{cat}}$  and  $K_{\text{m}}$  values revealed primary deuterium KIEs (Table 1) on both  $V_{\text{max}}$  (1.8) and  $V_{\text{max}}/K_{\text{m}}$  (2.2).

## References

- (1) Van Gunsteren, F. W.; Billeter, S. R.; Eising, A. A.; Hünenberger, P. H.; Krüger, P.; Mark, A. E.; Scott, W. R. P.; Tironi, I. G. *Biomolecular Simulation: The GROMOS96 Manual and User Guide* 1996, 1.
- (2) Guex, N.; Peitsch, M. C. *Electrophoresis* **1997**, 18, 2714.
- (3) DeLano, W. L. Schrödinger LLC [www.pymol.org](http://www.pymol.org) 2002, Version 1, <http://www.pymol.org>.
- (4) Anderson, V. E.; Cleland, W. W. *Biochemistry* **1990**, 29, 10498.
- (5) Gross, A.; Lewis, J. M.; George, M. J. *Am. Chem. Soc.* **1983**, 105, 7428.
- (6) Gu, X. R.; Yu, M.; Ivanetich, K. M.; Santi, D. V. *Biochemistry* **1998**, 37, 339.
- (7) Hamilton, C. S.; Greco, T. M.; Vizthum, C. A.; Ginter, J. M.; Johnston, M. V.; Mueller, E. G. *Biochemistry* **2006**, 45, 12029.
- (8) Miracco, E. J.; Mueller, E. G. *J. Am. Chem. Soc.* **2011**, 133, 11826.
- (9) McDonald, M. K.; Miracco, E. J.; Chen, J.; Xie, Y.; Mueller, E. G. *Biochemistry* **2011**, 50, 426.
- (10) Nurse, K.; Wrzesinski, J.; Bakin, A.; Lane, B. G.; Ofengand, J. *RNA* **1995**, 1, 102.
- (11) Ramamurthy, V.; Swann, S. L.; Paulson, J. L.; Spedaliere, C. J.; Mueller, E. G. *J. Biol. Chem.* **1999**, 274, 22225.
- (12) Tolbert, T. J.; Williamson, J. R. *J. Am. Chem. Soc.* **1996**, 118, 7929.
- (13) Van Lanen, S. G.; Kinzie, S. D.; Matthieu, S.; Link, T.; Culp, J.; Iwata-Reuyl, D. *J. Biol. Chem.* **2003**, 278, 10491.
- (14) Arthur, P. K.; Alvarado, L. J.; Dayie, T. K. *Protein Expr. Purif.* **2011**, 76, 229.
- (15) Ames, B. N.; Shigenaga, M. K.; Hagen, T. M. Assay of inorganic phosphate, total phosphate and phosphatases. *Methods Enzymol.* **1966**, 8, 115.
- (16) Hennig, M.; Scott, L. G.; Sperling, E.; Bermel, W.; Williamson, J. R. *J. Am. Chem. Soc.* **2007**, 129, 14911.
- (17) Stambaugh, R. L.; Wilson, D. W. *J. Chromatogr. A* **1960**, 3, 221.
- (18) Sambrook, J. In *Molecular Cloning: A Laboratory Manual*; Cold Spring Harbor: NY, 2001.
- (19) Strohalm, M.; Kavan, D.; Novák, P.; Volný, M.; Havlíček, V. *Anal. Chem.* **2010**, 82, 4648.
- (20) Mueller, E. G.; Ferré-D'Amaré, A. R. In *DNA and RNA Modification Enzymes: Structure, Mechanism, Function and Evolution*; Grosjean, H., Ed.; Landes Bioscience: Austin, TX, 2009, p 363.
- (21) Kammen, H. O.; Marvel, C. C.; Hardy, L.; Penhoet, E. E. *J. Biol. Chem.* **1988**, 263, 2255.
- (22) Gu, X. R.; Liu, Y. Q.; Santi, D. V. *Proc. Natl. Acad. Sci. U.S.A.* **1999**, 96, 14270.
- (23) Huang, L. X.; Pookanjanatavip, M.; Gu, X. G.; Santi, D. V. *Biochemistry* **1998**, 37, 344.
- (24) Kaya, Y.; Ofengand, J. *RNA* **2003**, 9, 711.
- (25) Phannachet, K.; Elias, Y.; Huang, R. H. *Biochemistry* **2005**, 44, 15488.
- (26) Hoang, C.; Ferré-D'Amaré, A. R. *Cell* **2001**, 107, 929.
- (27) Spedaliere, C. J.; Mueller, E. G. *RNA* **2004**, 10, 192.
- (28) Milligan, J. F.; Groebe, D. R.; Witherell, G. W.; Uhlenbeck, O. C. *Nucleic Acids Res.* **1987**, 15, 8783.
- (29) Macdonald, L. E.; Zhou, Y.; McAllister, W. T. *J. Mol. Biol.* **1993**, 232, 1030.